

Target Identification using Matrix Pencil

Final Report

Raviraj Adve
University of Toronto

Prepared By:
University of Toronto, Department of Electrical and Computer Engineering
10 King's College Road
Toronto, ON M5S 3G4

PWGSC Contract Number: W7707-135620
Contractor's date of publication: 31 March 2017
Technical Authority: Vincent Myers

Disclaimer: The scientific or technical validity of this Contract Report is entirely the responsibility of the Contractor and the contents do not necessarily have the approval or endorsement of the Department of National Defence of Canada.

Defence Research and Development Canada

Contract Report
DRDC-RDDC-2017-C194
August 2017

© Her Majesty the Queen in Right of Canada, as represented by the Minister of National Defence, 2017
© Sa Majesté la Reine (en droit du Canada), telle que représentée par le ministre de la Défense nationale,
2017

Target Identification Using Matrix Pencil

Raviraj S. Adve

Dept. of Electrical and Computer Engineering
University of Toronto
10 King's College Road
Toronto, Ontario, M5S 3G4, Canada

rsadve@comm.utoronto.ca

Final Report

March 31, 2017

Abstract

In underwater sonar systems, identifying targets from their signatures is an important, but, yet, open problem. The Matrix Pencil approach allows us to extract the modes (and mode amplitudes) of a decaying time domain signal. The main premise of this effort was that the modes are uniquely associated with individual targets and, hence, obtaining the modes should help target identification. This report presents the results of the use of the Matrix Pencil approach applied to the PondEX data sets provided by Defense Research and Development Canada (DRDC) Atlantic. The data set includes the sonar returns from a variety of targets and target-like objects from many along-track aspect angles and target orientations. As our results will show, in our analysis the Matrix Pencil approach is able to distinguish between two very different kinds of targets. We also discuss more cautionary results using comparisons of similar objects in different settings. However, we conclude that there is some promise in the notion of target discrimination and identification using the Matrix Pencil approach.

1 Introduction

An underwater synthetic aperture sonar (SAS) system provides high-resolution images of the seabed allowing for the detection of man-made objects such as mines, shells and debris. The goal of this project is to enhance discrimination between the objects detected, i.e., to improve the classification and identification of objects detected. To achieve this goal, we obtain class or object specific characteristics that, then, allow for this discrimination. Specifically, we use the Matrix Pencil approach [1,2]

Matrix Pencil is an example of model-based parameter estimation. The Matrix Pencil approach models the (sampled) time domain signal as a linear sum of complex exponentials; the goal is to find the parameters of the linear sum - the exponents, that are related to the modes, and the amplitudes (if required). While a sum-of-exponentials is a well-established model, Matrix Pencil differs from

other techniques in not requiring any statistical information; a single snapshot of collected data is adequate to execute the algorithm. The approach has been used in multiple applications such as indoor localization [3] and compensation for mutual coupling in adaptive processing [4].

The Matrix Pencil approach was tested using the PondEX data [5] made available by DRDC in March 2016. This report presents the results investigating the use of the Matrix Pencil in the context of the PondEX data sets. To avoid being unnecessarily repetitive, we present results for a subset of the targets: the aluminium pipe, the aluminium UXO shell placed on a flat sand/water interface (the “proud” setting) at 10m from the sonar and a rock (ROCK1 in the PondEX data set). For completeness, we begin with a review of the Matrix Pencil algorithm.

2 Matrix Pencil

In the Matrix Pencil approach, the time domain signal, here $x(t)$, is modeled as a sum of complex exponentials:

$$x(t) = \sum_{m=1}^M A_m e^{\zeta_m t}; \quad \zeta_m = \alpha_m + j\beta_m, \quad (1)$$

where $\zeta_m, m = 1, \dots, M$ represent the complex poles of the system. The real component of the mode, α_m denotes the mode attenuation while β_m , the imaginary component, denotes the mode frequency. Let $z_m = e^{\zeta_m \Delta t}$, where Δt is the sampling period. Then

$$x[n] = x(n\Delta t) = \sum_{m=1}^M A_m z_m^n; \quad n = 0, 1, \dots, N-1. \quad (2)$$

The goal is to estimate M , the number of poles, $z_m, m = 1, \dots, M$, the poles, and $A_m, m = 1, \dots, M$, the amplitudes of the poles.

The Matrix Pencil approach to estimate these parameters is as follows: we first choose the Matrix Pencil parameter $L \simeq N/2$ and form the $(N-L) \times (L+1)$ matrix \mathbf{X} defined as the

$$\mathbf{X} = \begin{bmatrix} x[0] & x[1] & \cdots & x[L-1] & x[L] \\ x[1] & x[2] & \cdots & x[L] & x[L+1] \\ \vdots & \vdots & \ddots & \vdots & \vdots \\ x[N-L-1] & x[N-L] & \cdots & x[N-2] & x[N-1] \end{bmatrix}, \quad (3)$$

We can now define the two $(N-L) \times L$ sub-matrices: matrices \mathbf{X}_0 and \mathbf{X}_1 as the first L and last L columns of \mathbf{X} , i.e. in MATLAB notation

$$\mathbf{X}_0 = \mathbf{X}(:, 1:L) \quad (4)$$

$$\mathbf{X}_1 = \mathbf{X}(:, 2:L+1). \quad (5)$$

Note that there is a single time-shift between these two matrices. Importantly, these two matrices can be written as

$$\mathbf{X}_0 = \mathbf{Z}_1 \mathbf{A} \mathbf{Z}_2, \quad (6)$$

$$\mathbf{X}_1 = \mathbf{Z}_1 \mathbf{A} \mathbf{Z}_0 \mathbf{Z}_2, \quad (7)$$

where,

$$\mathbf{Z}_1 = \begin{bmatrix} 1 & \cdots & 1 \\ z_1 & \cdots & z_M \\ \vdots & \ddots & \vdots \\ z_1^{(N-L-1)} & \cdots & z_M^{(N-L-1)} \end{bmatrix}_{(N-L) \times M} \quad (8)$$

$$\mathbf{Z}_2 = \begin{bmatrix} 1 & z_1 & \cdots & z_1^{L-1} \\ 1 & z_2 & \cdots & z_2^{L-1} \\ \vdots & \vdots & \ddots & \vdots \\ 1 & z_M & \cdots & z_M^{L-1} \end{bmatrix}_{M \times L}, \quad (9)$$

$$\mathbf{Z}_0 = \text{diag} [z_1 \ z_2 \ \cdots \ z_M], \quad (10)$$

$$\mathbf{A} = \text{diag} [A_1 \ A_2 \ \cdots \ A_M], \quad (11)$$

where $\text{diag}[\cdot]$ indicates a diagonal matrix with the corresponding entries on the diagonal. Based on Eqn. (7), our goal is to estimate the entries of the matrices \mathbf{Z}_0 and \mathbf{A} .

Consider the following formulation, called a ‘‘matrix pencil’’ (and hence the name of the algorithm):

$$\mathbf{X}_1 - \lambda \mathbf{X}_0 = \mathbf{Z}_1 \mathbf{A} [\mathbf{Z}_0 - \lambda \mathbf{I}] \mathbf{Z}_2. \quad (12)$$

Choosing $\lambda = z_m$, for some m , reduces the rank of the pencil by one. The estimates for z_m are, therefore, the *generalized eigenvalues* of the matrix pair $[\mathbf{X}_1, \mathbf{X}_0]$. This approach allows for an unambiguous estimation of the poles if

$$M \leq L \leq N - M. \quad (13)$$

Once we obtain the estimates of the modes in z_m , the attenuation factor $\alpha_m = \Re\{\log(z_m)/\Delta T\}$ and the mode frequency is given by $\beta_m = \Im\{\log(z_m)/\Delta T\}$ (here $\Re\{\cdot\}$ and $\Im\{\cdot\}$ denote the real and imaginary components of a complex number).

The amplitudes $A_m, m = 1, \dots, M$ can then be obtained by a least squares estimate [2] by solving

$$\begin{bmatrix} x[0] \\ x[1] \\ \vdots \\ x[N-1] \end{bmatrix} = \begin{bmatrix} z_1^0 & z_2^0 & \cdots & z_M^0 \\ z_1^1 & z_2^1 & \cdots & z_M^1 \\ \vdots & \vdots & \ddots & \vdots \\ z_1^{N-1} & z_2^{N-1} & \cdots & z_M^{N-1} \end{bmatrix} \quad (14)$$

3 Numerical Results

3.1 Illustrating the Matrix Pencil Approach

The PondEX data set, provided by DRDC, is described in [5] and in an explanation file that accompanies the data. The data comprises measurements of various targets, each in 9 different orientations and ranges. In some cases the same target is or is not buried. The transmitted signal is a linear FM covering the frequency range from 1 kHz to 30 kHz, i.e., this is relatively

low-frequency data. Furthermore, each of the 9 measurements, for the same target orientation and range, includes measurements from 2000 time samples for several cross-range positions. The sampling rate is 10^5 samples per second, i.e., $\Delta t = 1 \times 10^{-5}$ providing an unambiguous bandwidth of 50kHz. Since the data set has been pre-processed - and given the relatively flat spectrum of the transmit signal, *we do not attempt to deconvolve the transmitted signal from the measurements.*

The PondEX data is matched filter with the transmit pulse. This has an important implication. As Fig. 1 shows, the measured signal has both waxing and waning components. This does not fit the Matrix Pencil signal model that includes exponential signals that last “forever”. The model is best suited for decaying signals. In this effort, we bypassed this problem by modeling the signal from its peak value and beyond; Figure 2 plots the segment of signal used (from Fig. 1) in the Matrix Pencil model.

Figure 3 illustrates the efficacy of the Matrix Pencil approach. In this plot, we use $N = 96$ time samples (beginning, as described above, with the sample with maximum value). In the Matrix Pencil approach, we have $L = 51$ and $M = 40$. The plot overlays the original signal (as in Fig. 2) and the signal estimate obtained using the Matrix Pencil estimate of the amplitudes and poles in conjunction with the model in Eqn. (2). As is clear, the Matrix Pencil approach is remarkably accurate in its reconstruction of the signal.

We begin with examining the frequency response of the AL UXO Shell. Figure 4 plots the Fourier spectrum of the transmitted signal (red) and the measured signal for the aluminium UXO Shell at broadside. As the figure shows, the transmitted signal is almost constant over the transmission bandwidth, negating any possible benefits from deconvolution. Further, the return signal shows strong returns near 22kHz.

Figure 5 provides an additional confirmation that the Matrix Pencil approach captures the characteristics of the signal. The figure plots the frequency spectrum of the measure signal and overlays (by scaling the pole magnitudes so the comparison is easy to visualize) the mode frequencies and amplitudes. As can be seen, the locations of the mode frequencies (coupled with their magnitudes) corresponds well to the frequency spectrum.

The next set of figures investigates the consistency of the Matrix Pencil model as a function of cross-range position and aspect angle. Starting with the broadside signal at 0 degrees, the Figs. 6 and 7 respectively plot the frequency spectrum and the mode frequencies for five cross-range (along-track) positions. The figures plot the data for broadside and 4 positions symmetrically placed with respect to broadside. The 4 positions are spaced by 5 cross-range sample points, i.e., 12.5cm apart. Importantly, both the frequency spectra and the mode frequencies are consistent over all the cross-range positions.

A final comparison is across multiple aspect angles. The PondEX data set measures targets from various aspect angles. Figures 8 and 9 provide a comparison similar to 6 and 7. The plots cover three viewing angles (0 degrees or broadside and ± 20 degrees). As is clear, the main peak at about 22kHz is significantly attenuated. The mode frequencies are still consistent with the spectra, but show a wider variation amongst themselves.

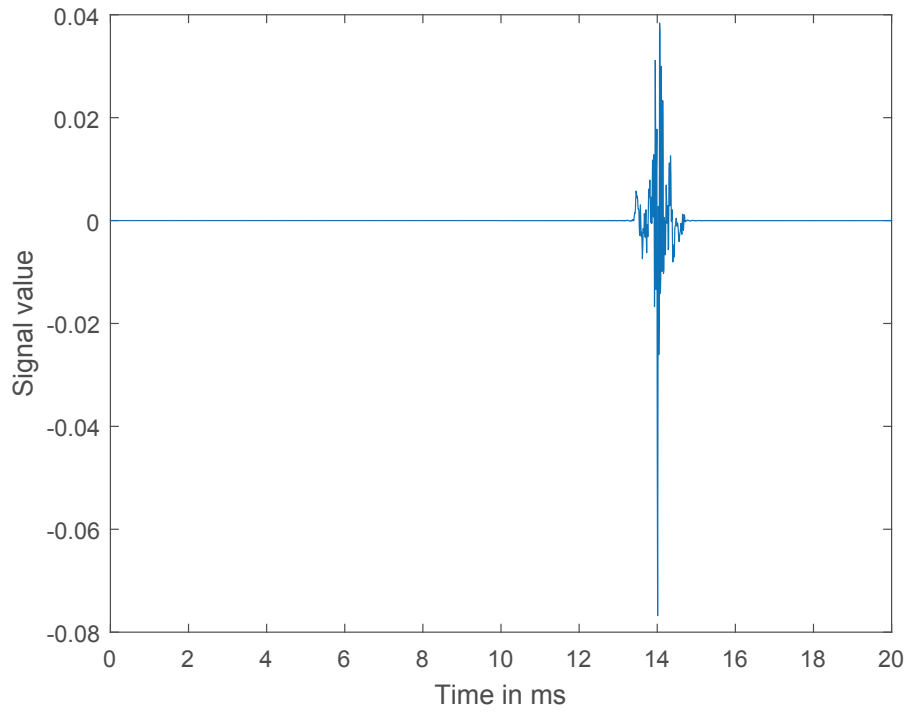


Figure 1: Complete measured signal at the center position. Aluminium UXO shell, proud at 10m.

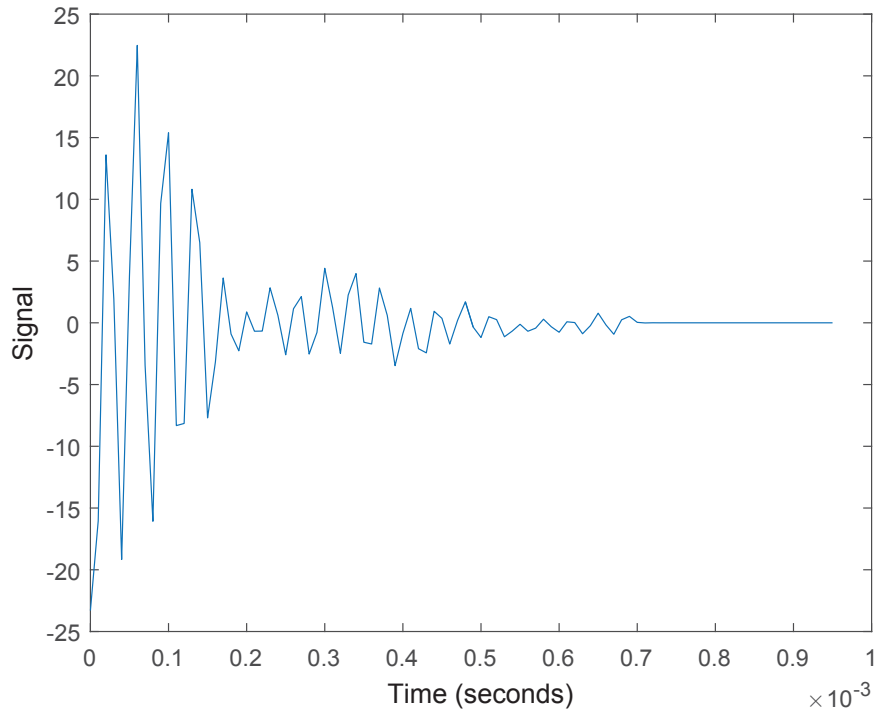


Figure 2: Segment of signal modeled using the Matrix Pencil approach. Aluminium UXO shell, proud at 10m.

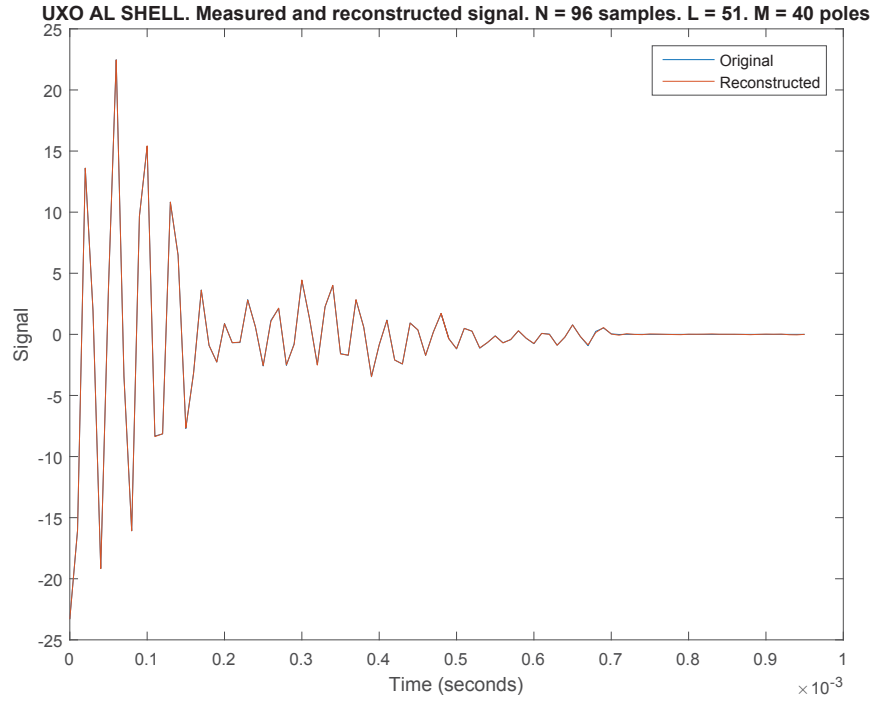


Figure 3: Comparing the original signal and the Matrix Pencil model. $N = 96, L = 51, M = 40$. Aluminium UXO Shell at Broadside.

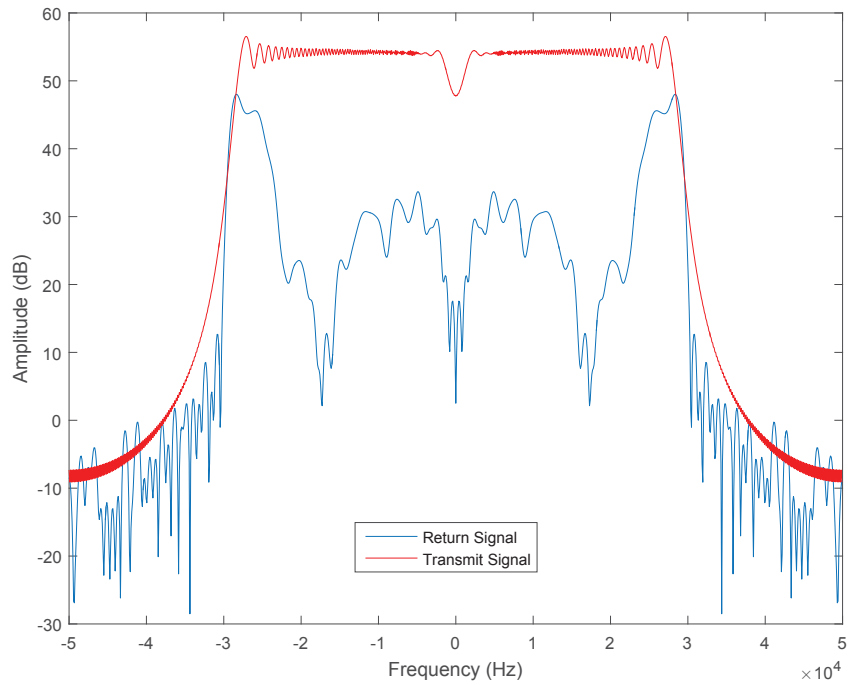


Figure 4: The Fourier spectra of the measured signal and the transmitted signal. Aluminium UXO Shell at Broadside.

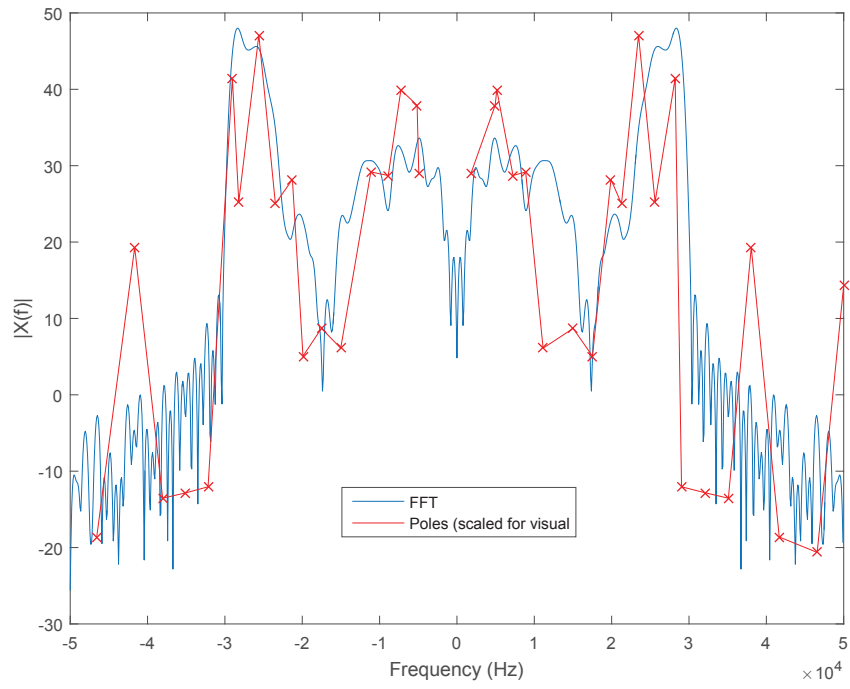


Figure 5: Comparing the frequency spectrum of the signal and the locations of the mode frequencies.

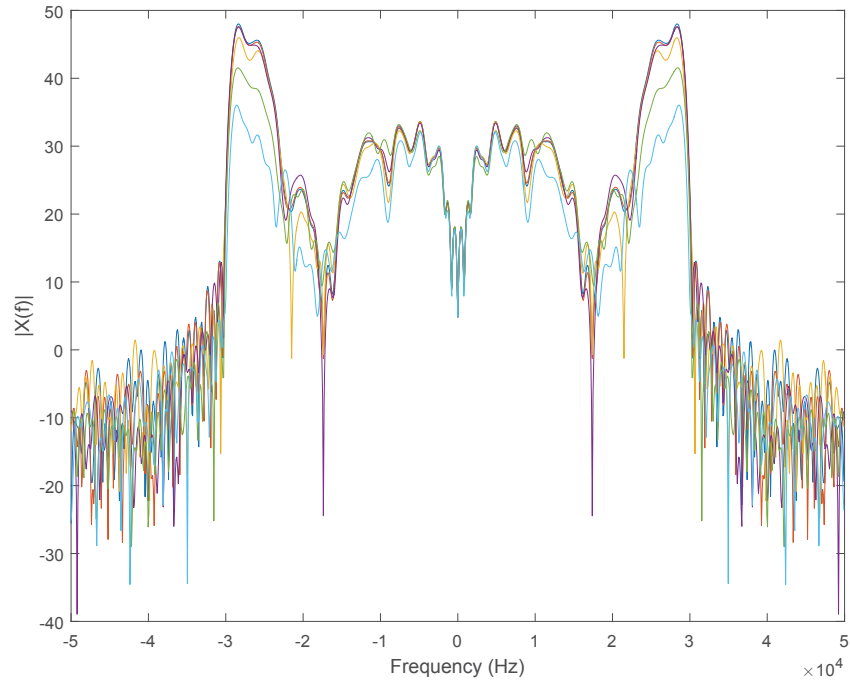


Figure 6: Frequency spectrum for five cross-range positions, centred at broadside, spaced 12.5cm (5 cross-range samples) apart. AL UXO Shell.

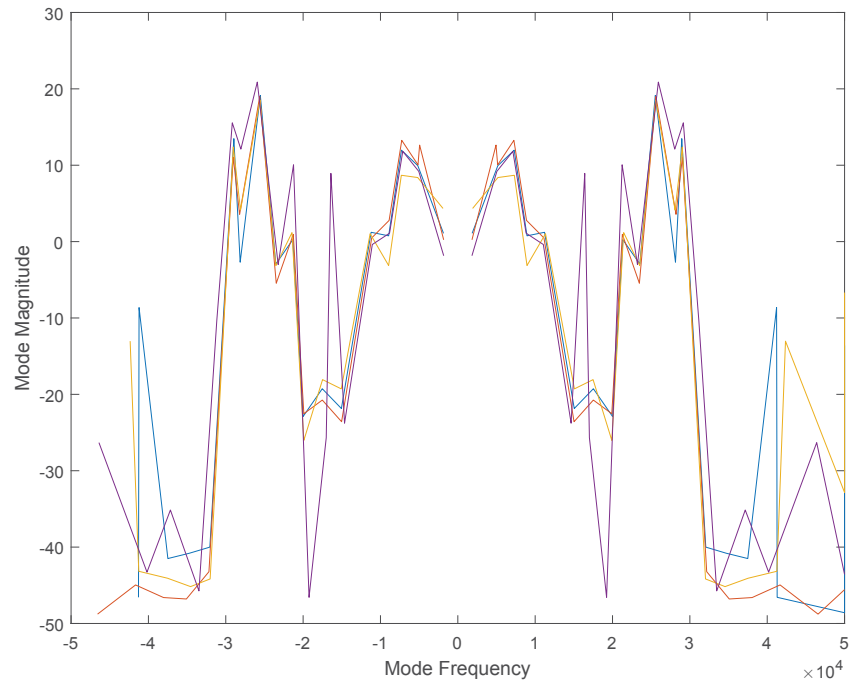


Figure 7: Mode frequencies for the same cross-range positions.

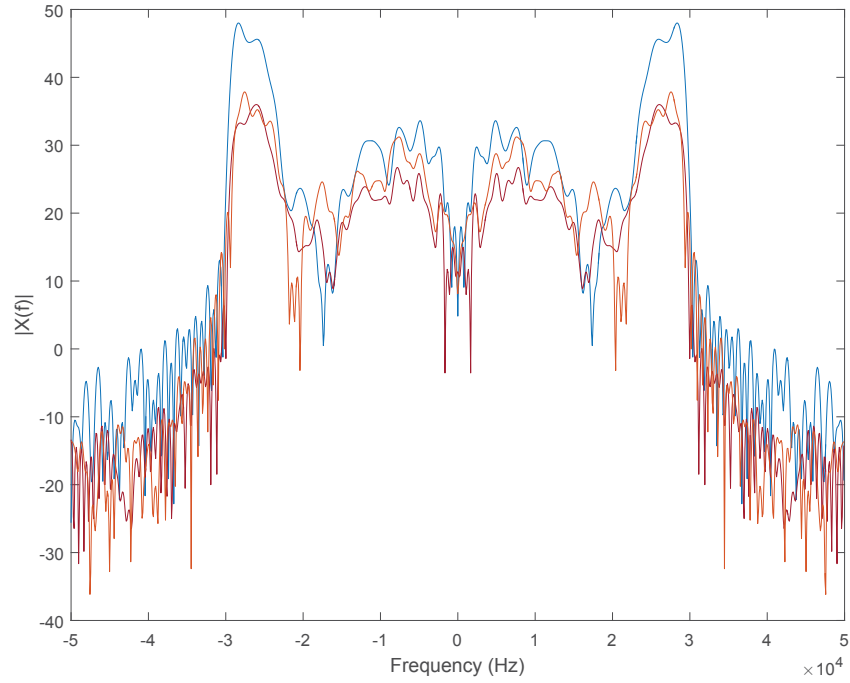


Figure 8: Frequency spectrum for three view angles. AL UXO Shell.

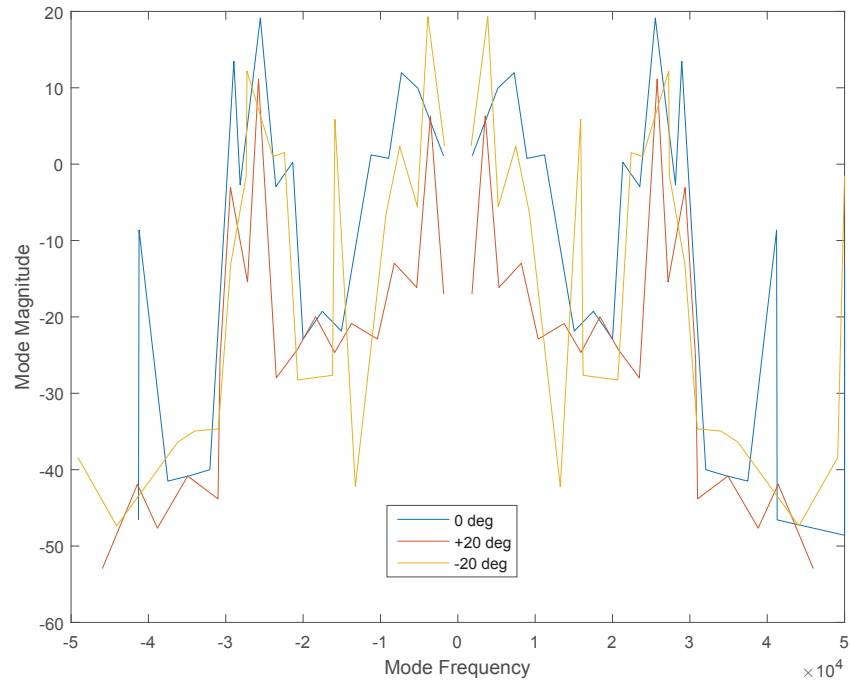


Figure 9: Mode frequencies for the same angle perspectives .

3.2 Using the Matrix Pencil for Discrimination

The results so far focus on proving the Matrix Pencil concept. We now illustrate the use of the Matrix Pencil approach for target identification, specifically discrimination between various targets. The Matrix Pencil approach associates with each return signal three length- M vectors: one each for the mode attenuation, frequency and amplitude. In this regard, comparisons require visualizing the results in three dimensions.

Figure 10 plots the $M = 40$ poles in three dimensional space (with the magnitude in dB), while Fig. 11 presents a similar plot for eleven cross-range positions. The eleven positions are chosen symmetrically placed across broadside, separated by 5cm (2 cross-range samples). As can be seen in Fig. 11, some of the modes cluster in 3D space while others diffuse. The diffusion complicates discrimination, though, it may be possible to exploit the pattern in which modes change over aspect angles.

Figure 12 provides are our first visual comparison of multiple targets, specifically the rock (x) and pipe (o). The figure plots (similar to Fig. 11) the modes in 3D space over eleven cross-range sample points (note that the along-track location of broadside may differ between the two targets). This figure is quite heartening since there is almost no overlap between the modes corresponding to the rock and the pipe. In fact, the modes for the pipe show far lower attenuation (due to the ringing inherent in a hollow pipe). This figure illustrates that, in the right circumstances, the Matrix Pencil algorithm clearly provides the discrimination we seek.

Figure 13 underlines this further, providing a similar comparison for the UXO shell and pipe. As in the previous figure, the modes corresponding to the two targets are largely disjoint (though the separation is not as clear as in the previous figure). This is further underlined in Fig. 14 which provides a similar comparison for the rock and shell. Here there is a substantial overlap of the two sets of modes and a simple visual inspection is inadequate to identify the targets.

Figure 14 shows that there is no easy discrimination between a rock and a shell. Figure 15 suggests that the main difference between the two is that the spectrum of the signal return from the rock shows less variation across frequencies than does that for the shell. Figure 16 shows that at least this information is captured in the modes as well. This suggests that one might need to recognize *patterns in the modes* to achieve the required discrimination.

Figure 17 presents the final result in this report and illustrates the use of the attenuation as a possible discriminant between certain types of targets. The figure plots the minimum value of the attenuations estimated by the Matrix Pencil algorithm as a function of cross-range. As is clear, the minimum attenuation amongst all modes is far smaller for the pipe than for any other target. This is consistent with Fig. 13.

4 Discussion and Conclusions

This effort investigated the use of the Matrix Pencil algorithm in discriminating between various targets in the PondEX data set. In the Matrix Pencil approach the return signal is modeled as a linear combination of exponential modes. The premise is that the modes will help identify the target.

This report has presented a selection of extensive results generate. The results show that discrimination is possible, but is not straightforward. In some cases, it is the mode attenuations that distinguish a target, while, in others, it is the modes frequencies identified by the Matrix Pencil

algorithm. However, this effort did not consider an automatic, machine-learning, based approach.

In summary, the results of this effort were promising and warrant a closer look. One could, for example, consider using the results from multiple aspect angles as training to help the classifier. Furthermore, the classifier could be seeded with some physical intuition such as target sizes, reflectivity, etc.

References

- [1] Y. Hua and T. K. Sarkar, "Matrix pencil method for estimating parameters of exponentially damped/undamped sinusoids in noise," *IEEE Transactions on Acoustics, Speech and Signal Processing*, vol. 38, pp. 814–824, May 1990.
- [2] R. S. Adve, O. M. Pereira-Filho, T. K. Sarkar, and S. M. Rao, "Extrapolation of time domain responses from three dimensional objects utilizing the matrix pencil technique," *IEEE Transactions on Antennas and Propagation*, vol. 45, pp. 147–156, January 1997.
- [3] K. Bayat and R. S. Adve, "Joint toa/doa wireless position location using matrix pencil," in *Vehicular Technology Conference, 2004. VTC2004-Fall. 2004 IEEE 60th*, vol. 5, Sept 2004, pp. 3535–3539 Vol. 5.
- [4] C. K. E. Lau, R. S. Adve, and T. K. Sarkar, "Minimum norm mutual coupling compensation with applications in direction of arrival estimation," *IEEE Transactions on Antennas and Propagation*, vol. 52, no. 8, pp. 2034–2041, Aug 2004.
- [5] K. L. Williams, S. G. Kargl, E. I. Thorsos, D. S. Burnett, J. L. Lopes, and M. Z. abd P. L. Marston, "Acoustic scattering from an aluminum cylinder in contact with a sand sediment: Measurements, modeling, and interpretation," *Journal of Acoustics Society of America*, vol. 127, pp. 3356–3371, 2010.

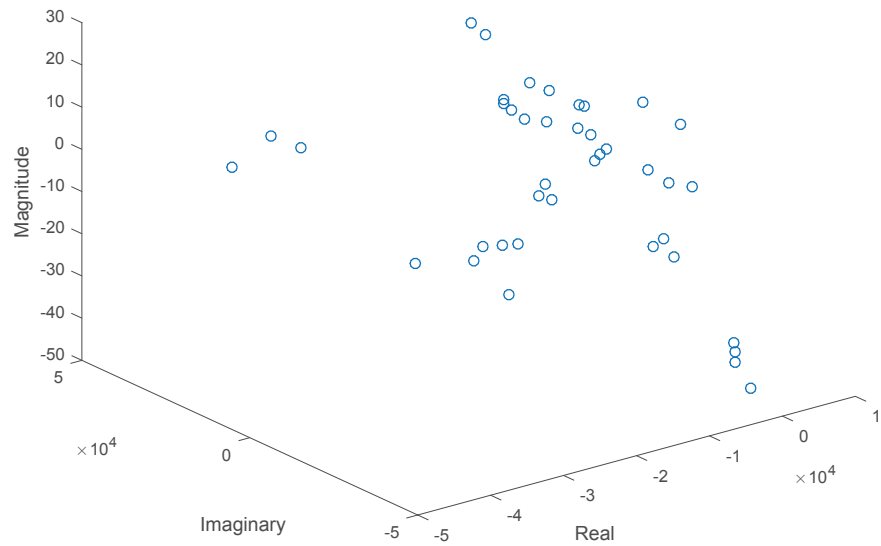


Figure 10: Modes in 3D space. Broadside. Each point marked represents a mode.

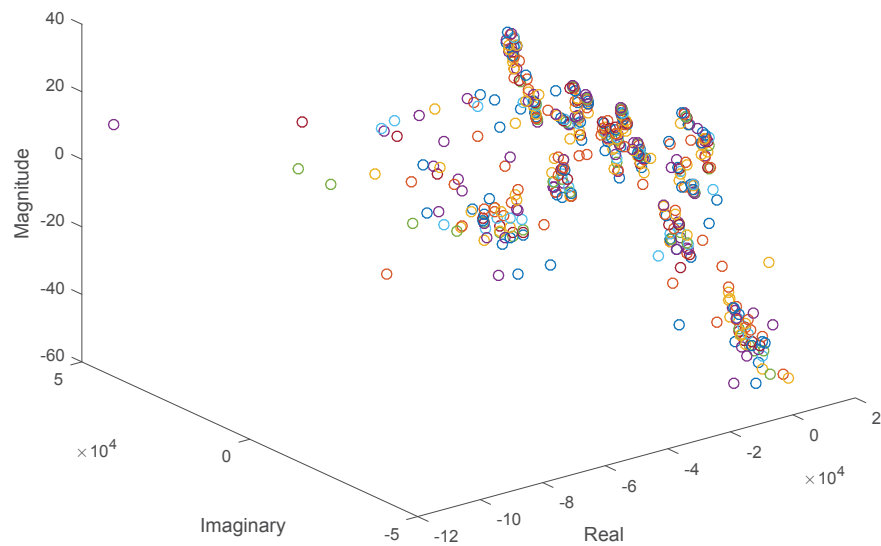


Figure 11: Modes in 3D space. Eleven cross-ranges centred at broadside 5cm apart (2 cross-range samples). Each point marked represents a mode.

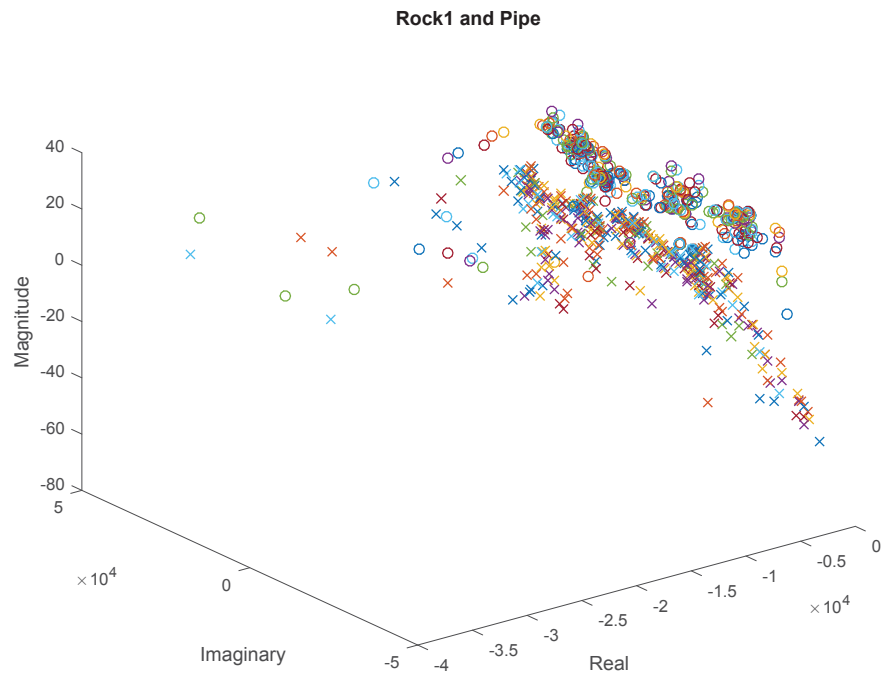


Figure 12: Comparing modes for the Rock and Pipe over several cross-ranges. Eleven cross-ranges centred at broadside 5cm apart (2 cross-range samples). Each point marked represents a mode.

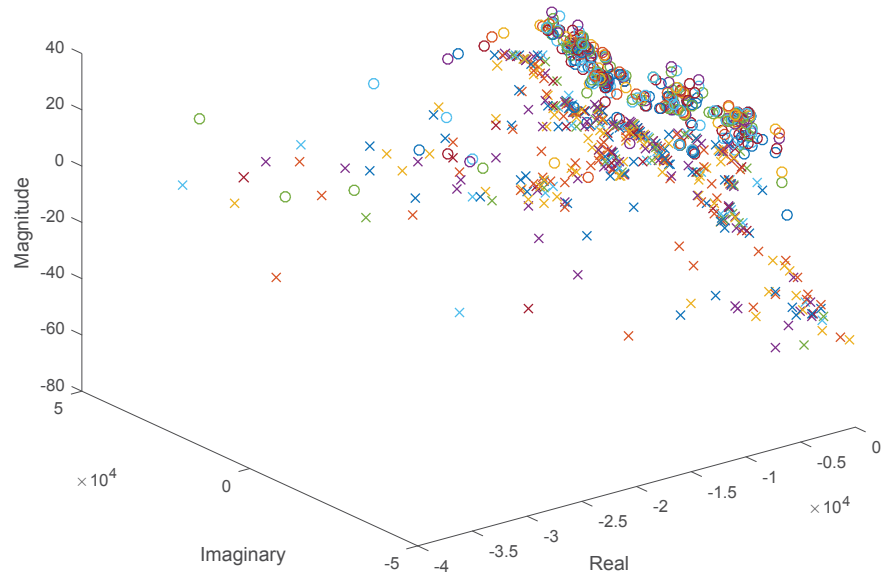


Figure 13: Comparing modes for the UXO Shell and Pipe over several cross-ranges. Eleven cross-ranges centred at broadside 5cm apart (2 cross-range samples). Each point marked represents a mode.

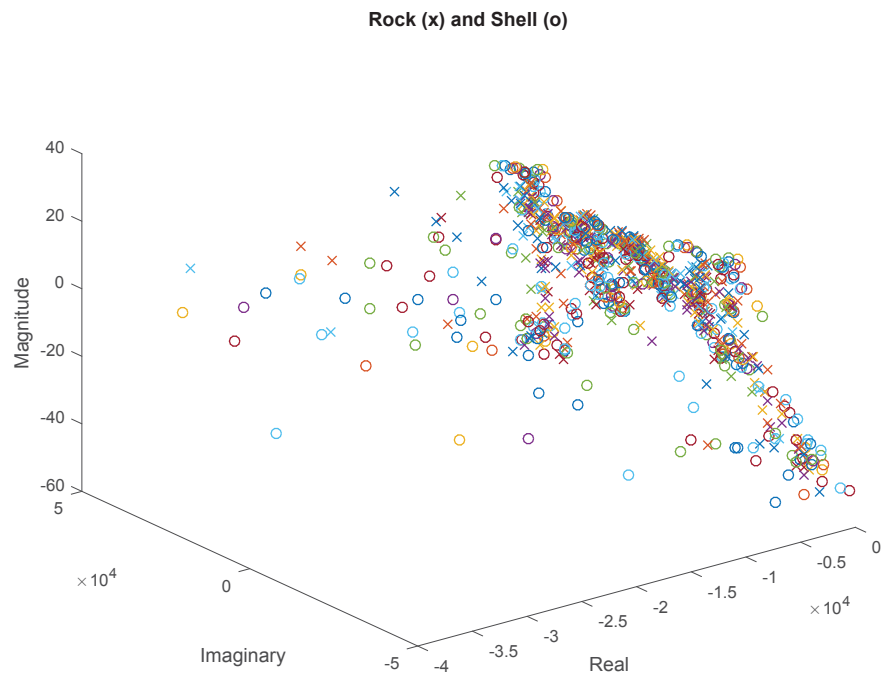


Figure 14: Comparing modes for the UXO Shell and Rock over several cross-ranges. Eleven cross-ranges centred at broadside 5cm apart (2 cross-range samples).

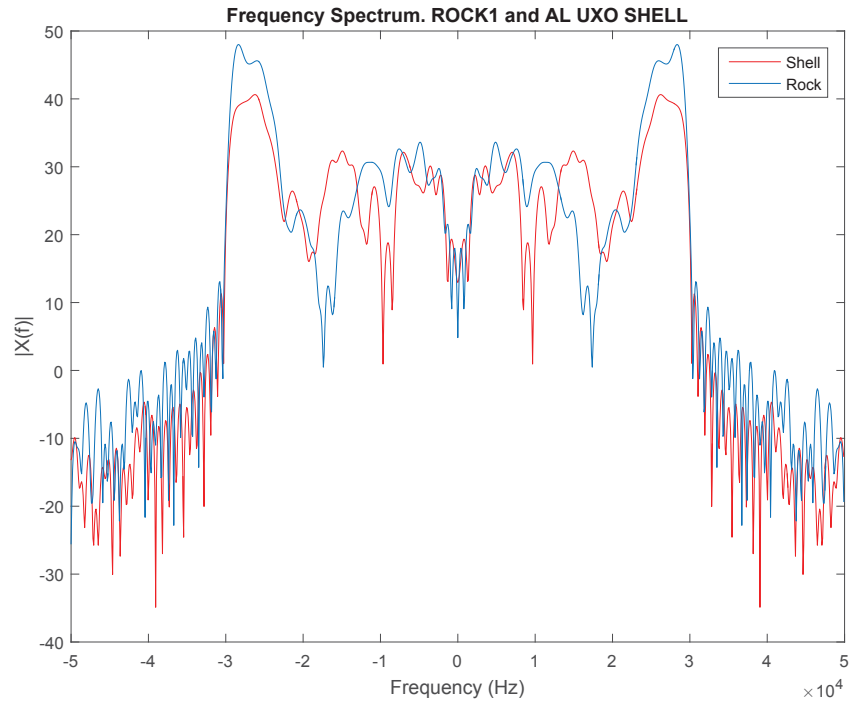


Figure 15: Spectrum of rock and shell. Broadside.

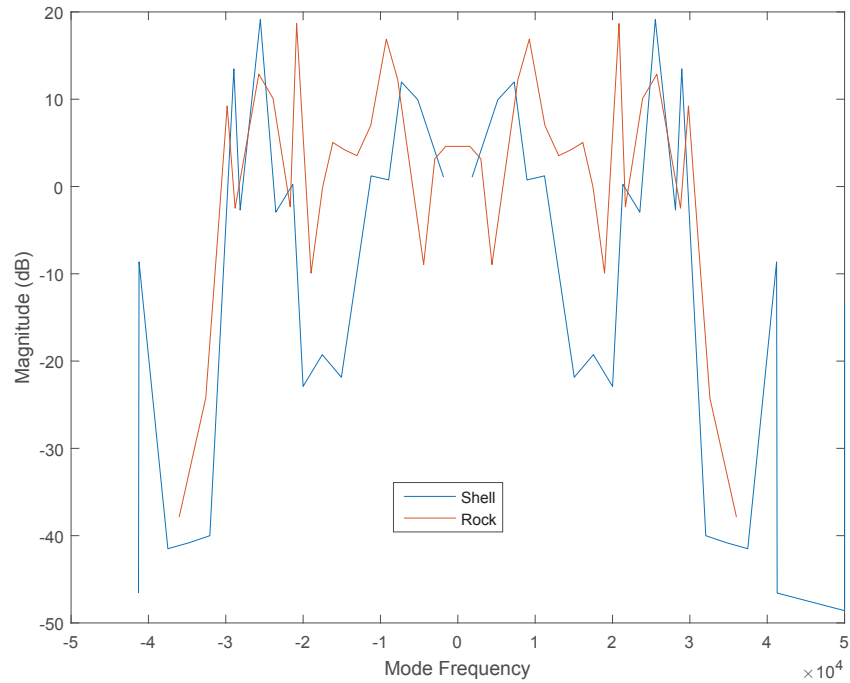


Figure 16: Spectrum of rock and shell. Broadside.

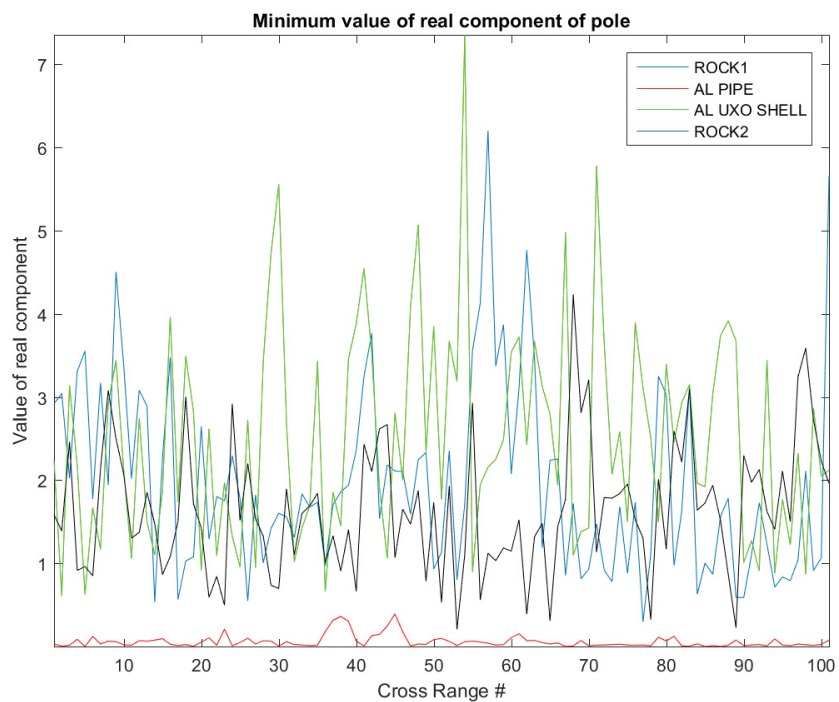


Figure 17: The min attenuation for several targets and cross-range samples.